RSC Advances

ROYAL SOCIETY OF CHEMISTRY

www.rsc.org/advances

Enhancement of thermoelectric power of PbTe:Ag nanocomposite thin films

Manju Bala [a], Srashti Gupta [b], Tripurari. S. Tripathi [c], Shikha Varma [d], Surya K. Tripathi [e], K. Asokan [a*], and Devesh K. Avasthi [a]*

[a] Materials Science Division, Inter University Accelerator Centre, Aruna Asaf Ali Marg, New Delhi-110067, India

[b] II. Physikalisches Institut Friedrich-Hund-Platz 137077 Göttingen, Germany

[c] Aalto University, Värmemansgränden 2, 02150 Esbo, Finland

[d] Insitute of Physics, Bhubaneshwar, Odisha-751005 , India

[e] Department of Physics, Panjab University, Chandigarh-160 014, India

* Corresponding Authors

Email: manjubala474@gmail.com, asokaniuac@gmail.com

ABSTRACT: Present study focuses on the enhancement of thermoelectric power of PbTe:Ag nanocomposite thin films, synthesized by thermal evaporation technique. Thermoelectric measurements were carried out from room temperature to 400 K. It is observed that Ag addition improves the thermoelectric power and crystalline nature of PbTe thin films. Synchrotron based X-ray diffraction was performed to confirm the phases of Pb-Ag-Te alloy. This was further reconfirmed by X-ray photoelectron spectroscopy (XPS) and showed the precipitation of Pb on the surface of PbTe:Ag films. The enhancement of thermoelectric power is thus attributed to the formation of $Ag_{2-x}Te$ alloy and the precipitation of Pb nanostructures on the surface. The origin of such enhancement is understood based on phenomenon of energy dependent filtering of charge carriers.

KEYWORDS: Thermoelectric material, Lead telluride, Thermoelectric power

1. INTRODUCTION

PbTe is a semiconductor with narrow bandgap (0.25 eV at 0 K). It is one of the most favorable thermoelectric materials for converting waste heat into electricity over a wide range of temperature (500-900 K)[1]. PbTe contains high concentration of charge carriers due to the presence of electrically active lattice defects as a consequence of its non-stoichiometric nature.

Samples containing excess of Pb with respect to the stoichiometric composition results in n-type, while those with excess of Te in p-type [2]. In general, the efficiency of a thermoelectric material is described in terms of a dimensionless parameter known as thermoelectric figure of merit (zT). It is expressed as, $zT=S^2T/\rho(\kappa_E+\kappa_L)$, where S is the thermoelectric power (Seebeck coefficient), ρ is the electrical resistivity, κ_E and κ_L are the electronic and lattice components of the thermal conductivity $(\kappa = \kappa_E + \kappa_L)$, respectively and T is the absolute temperature[3]. Thus for better thermoelectric performance, a large value for S, and small values of ρ and κ are required. It is a major challenge to increase zT by optimizing the parameters like S, ρ and κ_E because these are interrelated through the carrier concentration (n) [4]. In low dimensional systems, these parameters can be tuned independently. Since, last few decades many efforts have been made to enhance the thermoelectric properties of PbTe using various approaches. One of the approaches is the incorporation of nano-inclusions. These nano-inclusions enhance the thermoelectric power due to the low energy carrier filtering and/or act as phonon scattering centers and hence reduce the thermal conductivity [5-6]. Recently, there has been extensive research on PbTe, for the purpose of improving its thermoelectric energy conversion efficiency. Aaron and his group[7] achieved significant improvement in zT (1.4 at~700 K) of p-type PbTe by carefully controlling the carrier density through I doping. Joseph Heremans et al demonstrated that using Tl impurity in p-type PbTe, one can attain zT~1.5 at 773 K [8]. Similarly, Snyder et al reported zT~1.4 at 750 K in Na doped PbTe [9], and zT~1.8 at 850 K in Na doped $PbTe_{1-x}Se_x$ alloy[10]. Tavrina et al studied $Pb_{1-x}Bi_xTe$ system and observed the effect of the Bi element on thermoelectric properties of PbTe and reported the maximum values of thermoelectric power factor F = 37 μW/cm·K^2 for x ~ 0.0025 [11]. Beside all these elements, Ag has also been considered as one of the potential element to enhance the thermoelectric properties of PbTe. It has been reported that Ag in PbTe at low concentrations (< a few 10^{19} cm^{-3}) acts as a p-type dopant but at higher concentrations, i.e, in the range of 10^{19} cm^{-3}, results in n-type [12]. Yasutoshi et al showed that Ag addition in PbTe results in z ~1.38×10^{-3} K^{-1} with hole concentration of 1.34×10^{19}/cm^3 [13]. Martin et al. also demonstrated enhancement in thermoelectric power through the energy barrier scattering in Ag incorporated PbTe [5]. Dow et al studied the effect of Ag and Sb addition on the thermoelectric properties of PbTe and estimated the maximum zT=0.27 at 723 K for $Pb_{1-x}Ag_xTe$ alloys for x=0.1[14]. It may be noted that, so far most of the interest for PbTe composit was in the direction of bulk nanostructured materials. PbTe in the form of thin films have also been known to enhance

thermoelectric properties as compared to bulk PbTe due to quantum confinement effects[15]. Thermoelectric materials in the form of thin films are suitable for specific applications and there are only limited studies on thin films. Therefore, the purpose of the present study is to synthesize, characterize and investigate the effect of Ag addition on the thermoelectric power of PbTe thin films. The present work is motivated by earlier work of Dow et al, who showed that PbTe in the bulk form gives best thermoelectric results for 10% Ag, therefore it would be interesting to study the effect of Ag using 10 % and one higher concentration (20%) in PbTe thin films.

2. EXPERIMENTAL PROCEDURE

PbTe, and Ag incorporated PbTe thin films were synthesized by thermal evaporation method on quartz substrates at a pressure of ~2×10^{-5} mbar. For convenience hereafter, the pristine PbTe, 10 % and 20 % Ag added PbTe thin films will be referred as PbTe, PbTe:10Ag and PbTe:20Ag, respectively. Rutherford backscattering spectrometry (RBS) was performed using 3 MeV He^{+} ions at scattering angle of 165^{o} at IUAC, New Delhi for compositional studies. Rutherford manipulation program (RUMP) simulation code was used to simulate the experimental RBS spectra. X-ray diffraction (XRD) measurements were performed at grazing incident angle of 2^{o} to identify the crystalline phases in the films using a Bruker D8 advance diffractometer with Cu Kα (1.5406 Å) X-ray source at a scan speed of 0.5^{o}/min. High resolution XRD measurement was also carried out at synchrotron radiation facility of KEK (Japan) using 13.9 keV energy. X-ray photoelectron spectroscopy (XPS) study was performed for the elemental composition on the surface of the sample using a VG instrument having system resolution ~0.9 eV with a Mg source, at IOP, Bhubaneswar. The surface morphology of thin film was examined using scanning electron microscopy (SEM) and atomic force microscopy (AFM) in tapping mode. The electrical resistivity (ρ) and thermoelectric power (S) of the films were measured in the temperature range (300-400K) using a standard DC four probe technique and bridge method[16], respectively. The Hall effect measurements were carried out using a magnetic field of 0.57 Tesla at room temperature to evaluate carrier density and mobility.

3. RESULTS AND DISCUSSION

3.1 Compositional Study

RBS spectra (with RUMP simulation) of the three thin films PbTe, PbTe:10Ag and PbTe:20Ag are shown in Figure 1. The simulation suggests that the thickness of these films are ~ 60-70 nm. The estimated atomic percentage of Pb, Te, Ag and O ions in these films are given in Table 1. The atomic percentages of Pb and Te exhibit deviations from expected stoichiometry and excess of Te as given in table 1. The Ag contents are found to be ~ 11.6 at % and 19.3 at % in PbTe:10Ag and PbTe:20Ag, respectively. The RUMP simulation also shows the presence of ~ 17- 19 at % of oxygen in all films. Such O contamination is known to occur during thermal evaporation process[18].

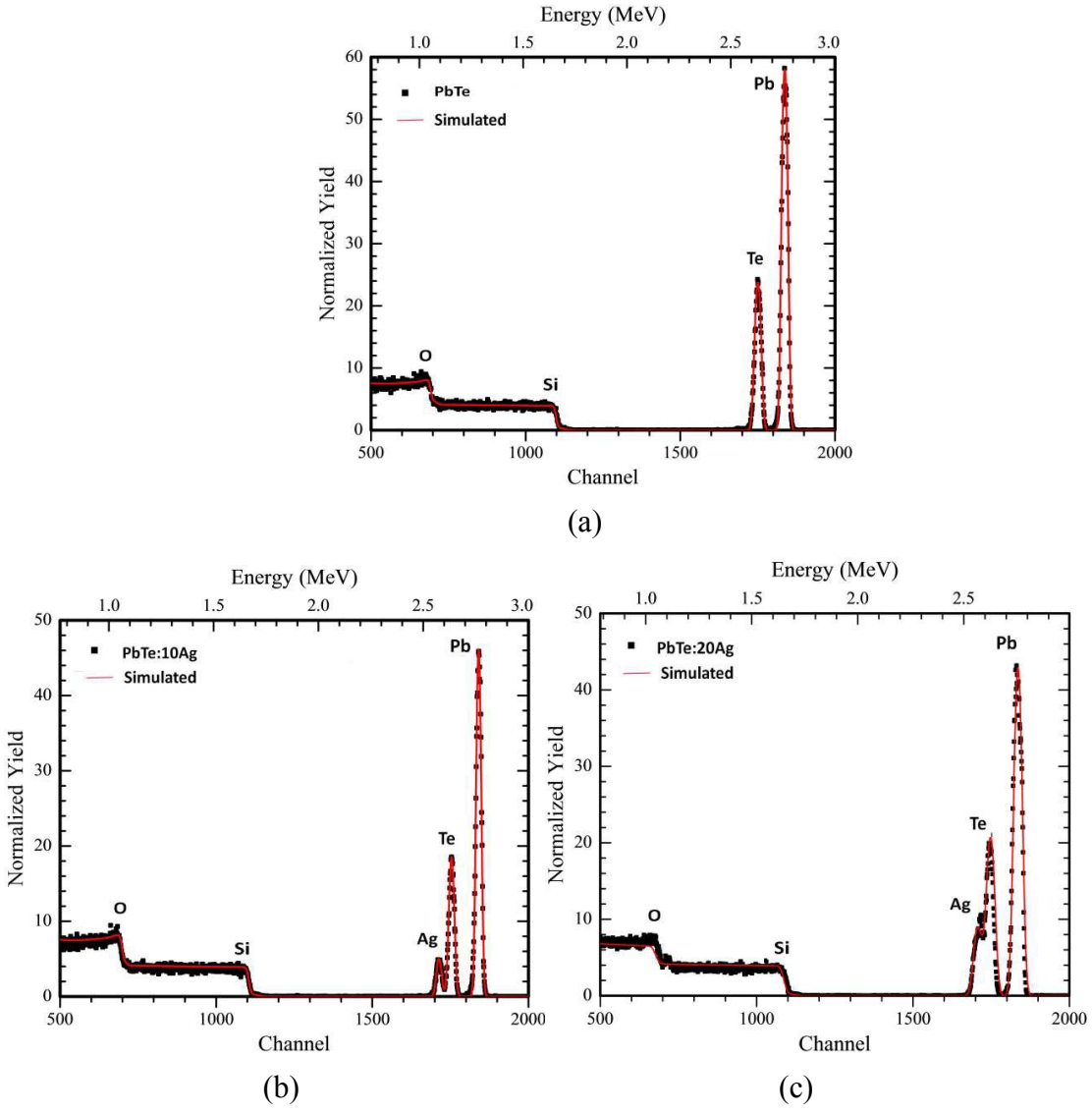

Figure 1. The dots show the experiment data and continuous line corresponds to simulation by RUMP for (a) PbTe (b) PbTe:10Ag and (c) PbTe:20Ag thin films.

Table 1: Elemental compositions of PbTe, PbTe:10Ag and PbTe:20Ag thin films determined by RBS simulation.

Sample	Pb (at%)	Te (at%)	Ag (at%)	O (at%)
PbTe	**39.6**	**41.6**	**0**	**18.8**
PbTe:10Ag	**34.4**	**37.1**	**11.6**	**16.9**
PbTe:20Ag	**31.1**	**32.6**	**19.3**	**17.0**

3.2. Phase Study

The XRD spectra of PbTe, PbTe:10Ag and PbTe:20Ag films are shown in Figure 2(a). The characteristic peaks in the spectra indicate the crystal structure of face centred cube (fcc) NaCl-type. The highest intensity peak at $2\theta=27.57^{o}$ suggests a preferential growth along the (200) planes. The XRD spectra of PbTe:10Ag and PbTe:20Ag are similar to that of PbTe. No peak corresponding to Ag or its alloys is observed in XRD spectra. An increase in peak intensity and decrease in full width half maxima (FWHM) was observed in the spectra (Figure 2(b)) for PbTe:10Ag and PbTe:20Ag which imply an increase in the crystalline nature of PbTe on adding Ag. The average size of the crystallites in thin films were determined by using Scherrer equation, $L = K\lambda/\beta \cos\theta_B$, where L is crystallite size, K is a constant, λ is the wavelength of the x-ray, β is the half width of a diffraction peak, and θ_B is the diffraction angle. It is observed (Figure 3) that the grain size increases with Ag addition but not in regular manner. The estimated values of grain size are ~18.6 nm, 22.2 nm and 21.4 nm, respectively, for PbTe, PbTe:10Ag and PbTe:20Ag corresponding to (2 0 0) plane, as given in Table 2. The increase in grain size in PbTe:10Ag and PbTe:20Ag films may be due to the diffusion of Ag-ion into PbTe during evaporation, which provide nucleation site for grain growth and hence increases the crystallinity [17]. XRD spectra obtained using lab source (Cu Kα) for PbTe:Ag samples do not show any peak of Ag or its alloy. Therefore high resolution XRD measurement was carried out at synchrotron radiation facility at KEK (Japan) using 13.9 keV energy to detect the small contents of Ag and its alloy. Synchrotron XRD spectra of PbTe:20Ag film showed two extra peaks at $2\theta=5.84^{o}$ and 7.02^{o} (Figure 4) which corresponds to either Ag_7Te_4 (JCPDS75-1022), $Ag_{1.85}Te$ (JCPDS108-

1186) or Ag_5Te_3 (JCPDS86-1168). Thus, these spectra suggest the presence of $Ag_{2-x}Te$ phase in PbTe:Ag samples. The Ag-Te alloy formation is further confirmed by X-ray photoelectron spectroscopy (XPS).

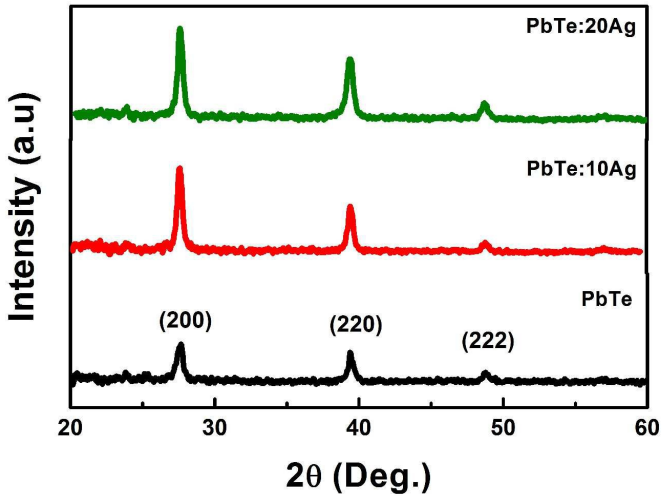

(a)

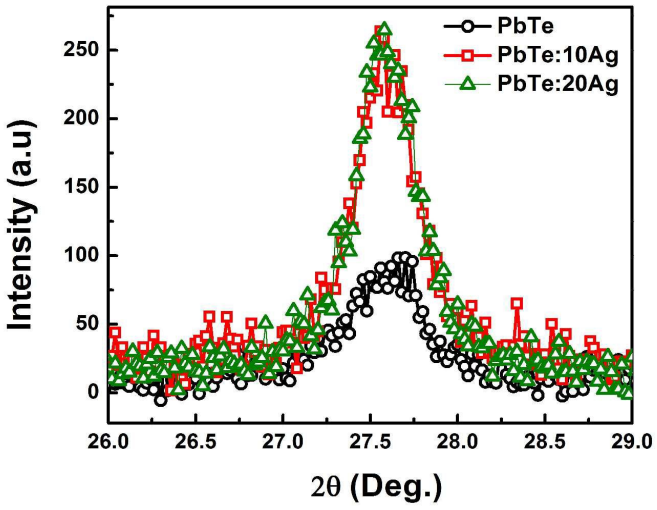

(b)

Figure 2 XRD spectra of thin films of PbTe, PbTe:10Ag and PbTe:20Ag. (a) Spectra showing 2θ from 20 to 60º and (b) Closer view of the peak corresponding to (2 0 0) plane

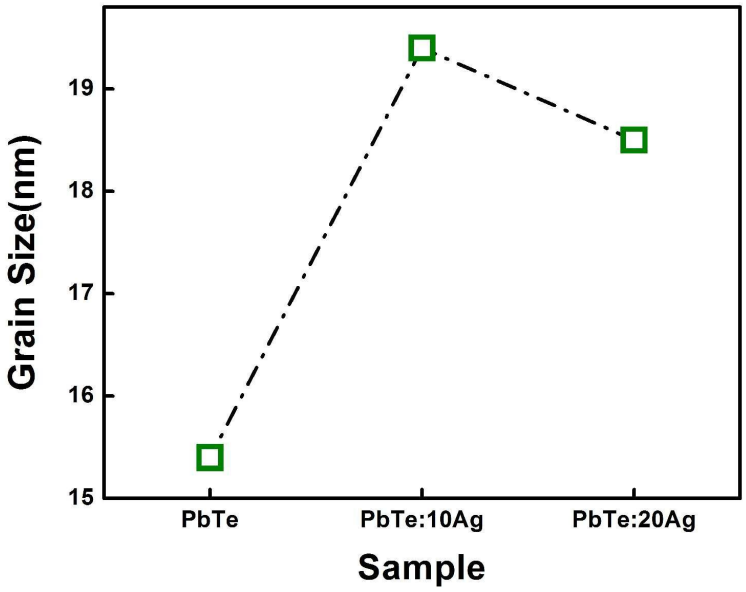

Figure 3 Variation of grain sizes of PbTe on adding Ag in PbTe thin films

Table 2: Peak position, FWHM and grain size of PbTe, PbTe:10Ag and PbTe:20Ag thin films

Sample	Peak position 2Θ (Deg.)	FWHM (Deg)	Crystallite size (nm)
PbTe	27.58	0.43	~ 18.62
PbTe:10Ag	27.58	0.36	~ 22.20
PbTe:20Ag	27.58	0.38	~ 21.38

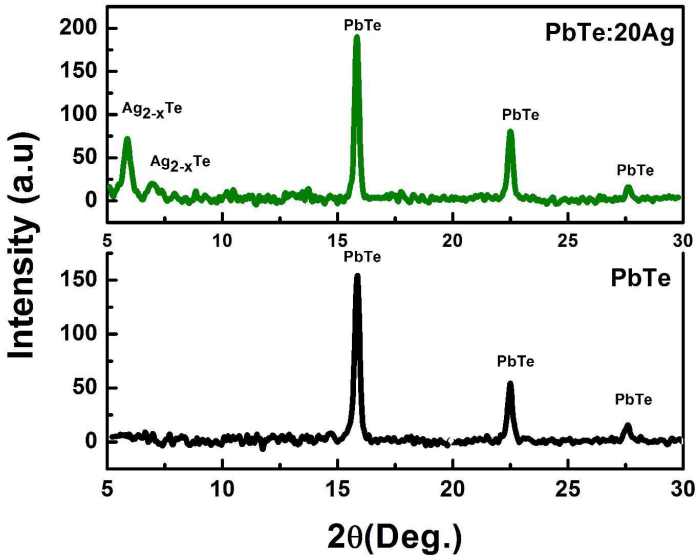

Figure 4 Synchrotron XRD spectra of PbTe and PbTe:20Ag measured at KEK (Japan) using energy of 13.9keV.

The XPS spectra of PbTe, PbTe:10Ag and PbTe:20Ag films are shown in Figure 5. For PbTe film two groups of peaks assigned to Pb ($4f_{7/2}$) and Pb ($4f_{5/2}$) are shown in the Figure 5(a). Each group contains a shoulder peak on the lower binding energy side. Deconvoluting the Pb ($4f_{7/2}$) peak by curve fitting distinguishes two components, one at 137.9 and another at 139.1 eV which correspond to PbTe (Pb^{2+}) and PbO (Pb^{2+}) [18] respectively. Te ($3d_{5/2}$) and Te ($3d_{3/2}$) peaks (Figure 5(a)) centered at 576.1eV and 586.5eV respectively, corresponding to TeO_2 (Te^{4+}). Two additional peaks at 572.4eV ($3d_{5/2}$) and 582.7eV ($3d_{3/2}$) are also observed corresponding to PbTe (Te^{2-}). The XPS data show the existence of PbO, TeO_2 and PbTe on the surface of the pristine film. This assignment is in good agreement with the data of Huizhen et al [19]. Figure 5(b) shows the XPS spectra of PbTe:10Ag. The Pb peaks corresponding to PbTe and PbO are found to be nearly at the same position as in pristine film. A shoulder peak on the higher binding energy side of Te peak is observed. Deconvoluting the Te ($3d_{5/2}$) peak distinguishes two components at 571.9 eV and 573.0eV, corresponding to PbTe (Te^{2-}) and $Ag_{2-x}Te$ (Te^{2-}) respectively. Along with these peaks, the TeO_2 (Te^{4+}) ($3d_{5/2}$) peak also appears at 575.9eV. XPS data reveal the presence of Ag in the PbTe:10Ag (Figure 5(b)). The peaks for Ag ($3d_{5/2}$) and Ag ($3d_{3/2}$) are observed. Deconvoluting the Ag ($3d_{5/2}$) peak gives two component at 368.2 and 368.9eV which correspond to Ag element (Ag^0) and $Ag_{2-x}Te$ (Ag^+) [20]. Similar components for Pb, Te and Ag are observed

in PbTe:20Ag (Figure 5(c)) confirming the existence of Ag-Te alloy ($Ag_{2-x}Te$) along with PbO, PbTe, TeO_2 and Ag element on the surface. The peak intensities of Pb, Te and Ag for all the films are shown in Figure 6. While the peak intensity of Pb is higher for Ag added PbTe films, the peak intensity of Te is lower compared to PbTe. This indicates that precipitation of Pb on the surface. A binding energy shift towards higher energy side for Pb in case of PbTe:10Ag can be seen in Figure 6(a). This is probably a final state effect and may be caused by very small sized nanostructures along with larger sized nanostructures. These explanations are supported by the morphological studies using AFM and SEM with EDS.

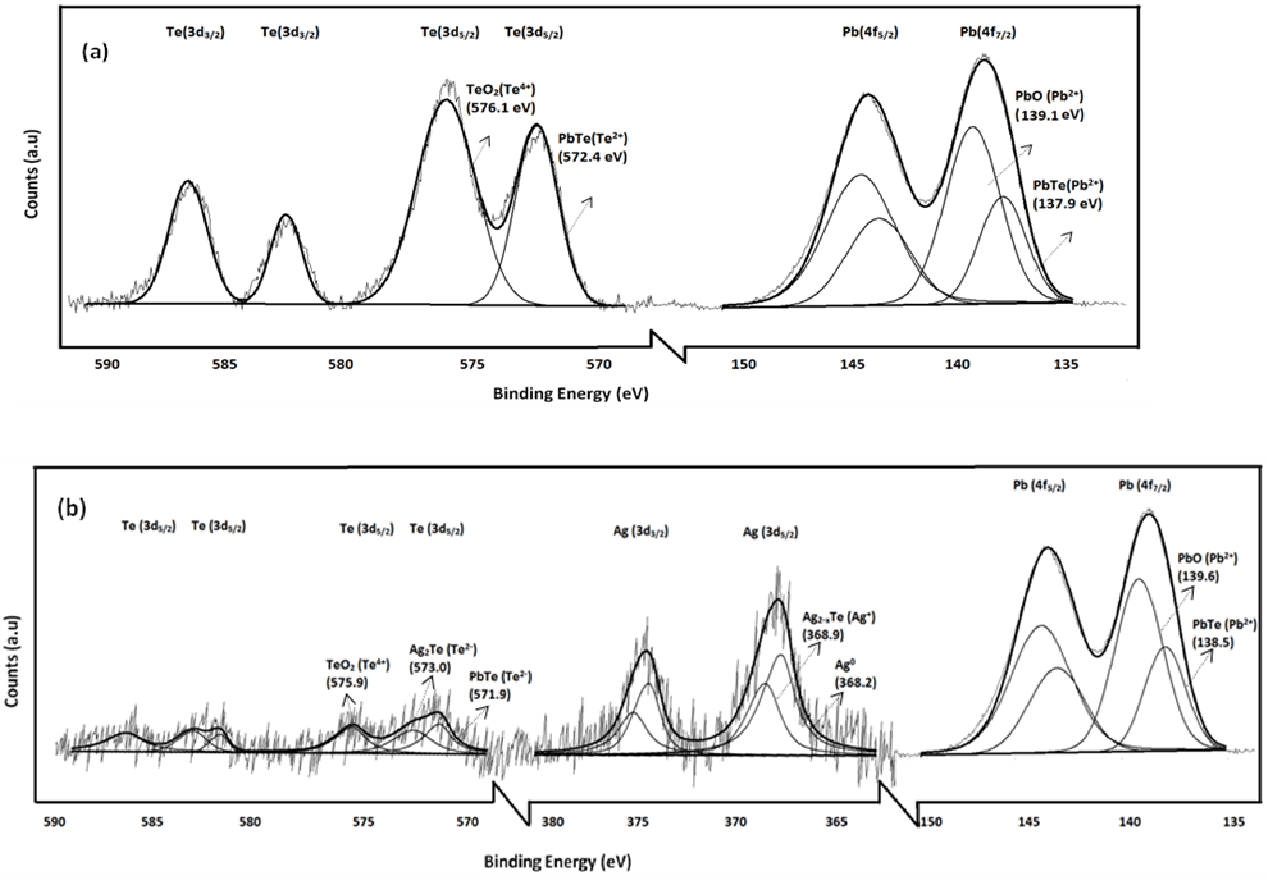

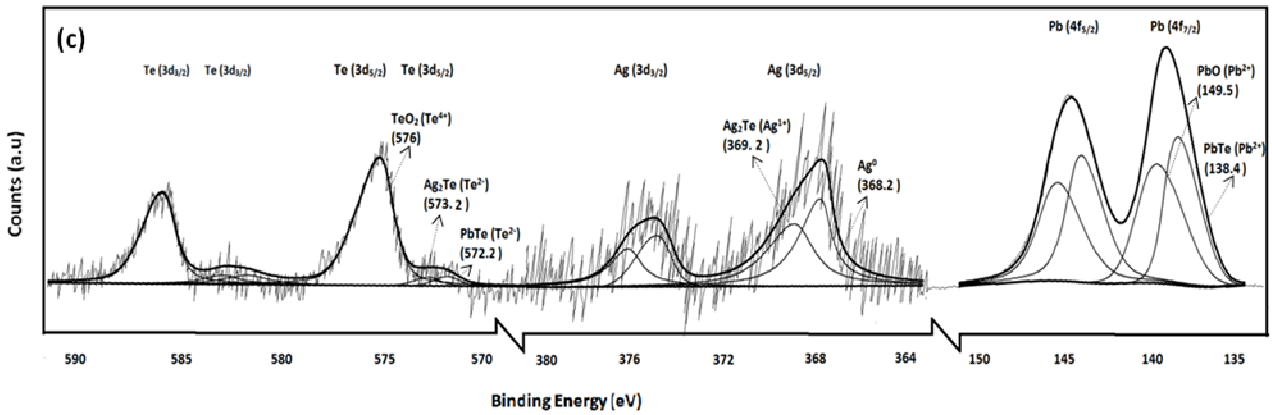

Figure 5: XPS spectra of (a) PbTe (b) PbTe:10Ag (c) PbTe:20Ag corresponding to 3d peaks of Te 4f peaks of Pb and 3d peaks of Ag.

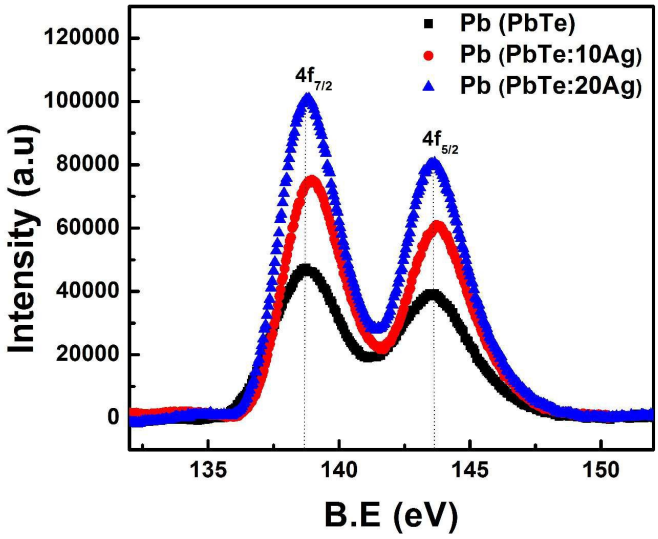

(a)

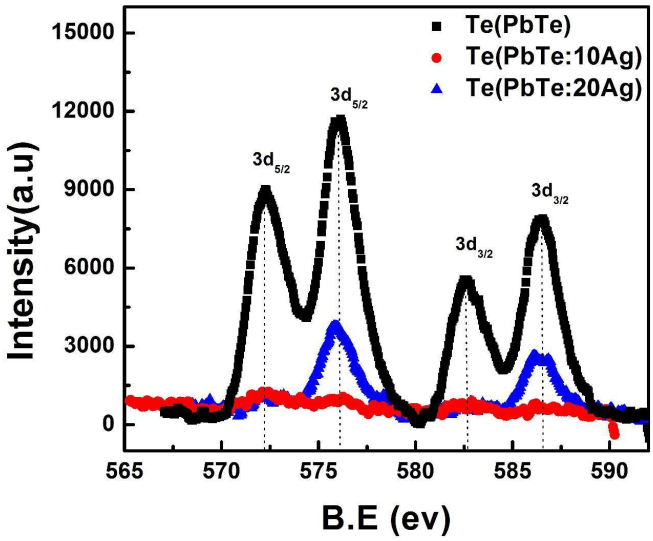

(b)

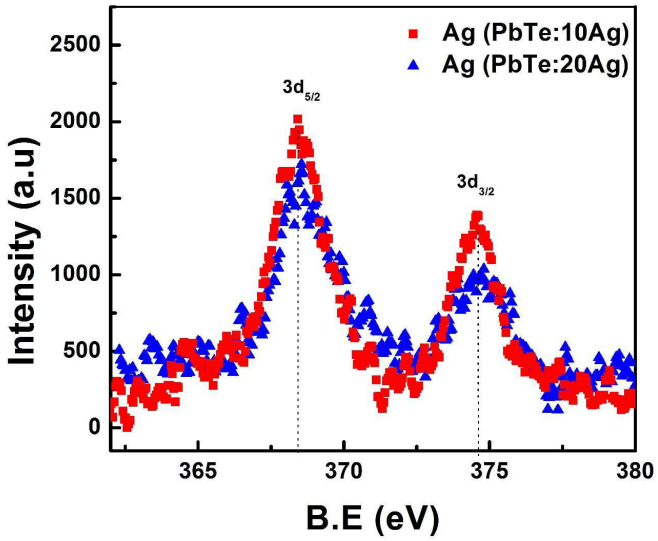

(c)

Figure 6. Comparison of peak intensities of PbTe, PbTe:10Ag and PbTe:20Ag films at (a) Pb 4f, (b) Te 3d, and (c) Ag 3d edges.

3.3. Morphological Study

Figure 7 shows the AFM images of PbTe, PbTe:10Ag and PbTe:20Ag films and it is evident that Ag addition results in significant change in the surface morphology. Nanosize islands like nanostructures of dimension ~60 nm×150 nm are seen in PbTe:10Ag thin films. For PbTe:20Ag thin film these islands become much more dense and their dimensions are found to be ~ 50 nm×120 nm (i.e smaller than PbTe:10Ag thin film). Surface roughness of the PbTe thin film is ~52.4 nm which reduced to 31.6 nm and 41.7 nm for PbTe:10Ag and PbTe:20Ag thin films, respectively.

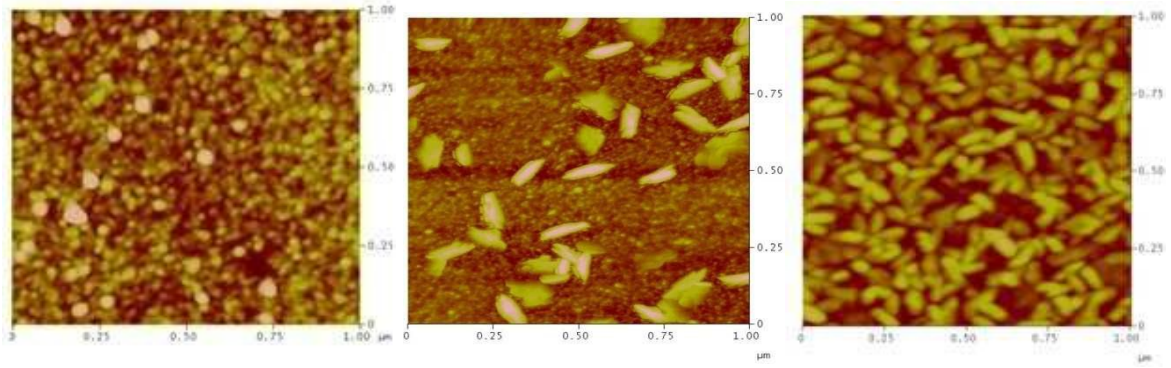

(a) PbTe (b) PbTe:10Ag (c) PbTe:20Ag

Figure 7. AFM images of (a) PbTe (b) PbTe:10Ag (c) PbTe:20Ag films

Surface morphology and the elemental composition in nanostructures formed in Ag added PbTe thin films were checked using SEM equipped with an energy dispersive spectrometer (EDS). Figure 8 (a), (b) and (c) shows the SEM images of PbTe, PbTe:10Ag, and PbTe:20Ag films respectively. Images acquired from SEM are consistent with AFM images. The composition values at two different points A (where nanostructures are present) and B (on the flat region) on each set of sample is given in Table 3. From EDS study, it is observed that the nano-size islands like nanostructures contain Pb, Te, Ag and they are Pb rich while everywhere else Pb and Te are present in 1:1 (within 11 %) stoichiometry. This indicates that the nanostructures are formed due to the presence of metallic Pb inclusions, possibly because of Ag ions which bind preferentially with Te by liberating Pb atoms to precipitate out [21].

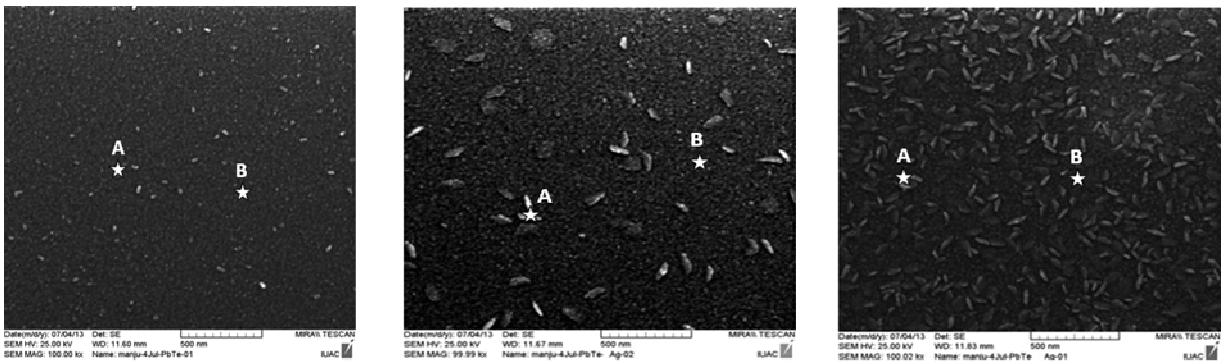

(a) PbTe (b) PbTe:10Ag (c) PbTe:20Ag

Figure 8. SEM images of (a) PbTe (b) PbTe:10Ag (c) PbTe:20Ag thin films

Table 3: Elemental compositions of PbTe, PbTe:10Ag and PbTe:20Ag thin films determined by EDS

	A				B			
Sample	**Pb (At%)**	**Te (At%)**	**Ag (At%)**	**Pb/Te**	**Pb (At%)**	**Te (At%)**	**Ag (At%)**	**Pb/Te**
PbTe	**52.3**	**47.6**	**0**	**1.09**	**52.6**	**47.3**	**0**	**1.11**
PbTe:10Ag	**50.1**	**37.6**	**12.3**	**1.33**	**49.2**	**44.2**	**6.6**	**1.11**
PbTe:20Ag	**45.7**	**35.8**	**18.5**	**1.27**	**45.2**	**43**	**11.8**	**1.05**

3.4 Transport and Thermoelectric Measurements

The variation of the thermoelectric powers (S) of PbTe, PbTe:10Ag and PbTe:20Ag nanocomposite films in the temperature range of 300 to 400 K are shown in Figure 9(a). The measured thermoelectric power at 400 K for PbTe, PbTe:10Ag and PbTe:20Ag film are ~288, ~376 and ~317 μV/K respectively. The measured value of thermoelectric power of PbTe sample is in accordance with the previous reports[22]. The thermoelectric power of PbTe:10Ag and PbTe:20Ag nanocomposite films are found to be ~30 % and ~10 % higher than the PbTe thin film, respectively.

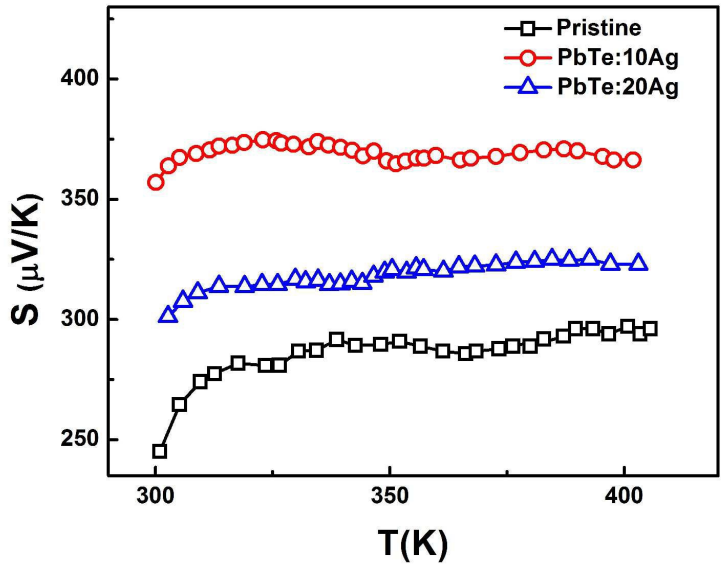

(a)

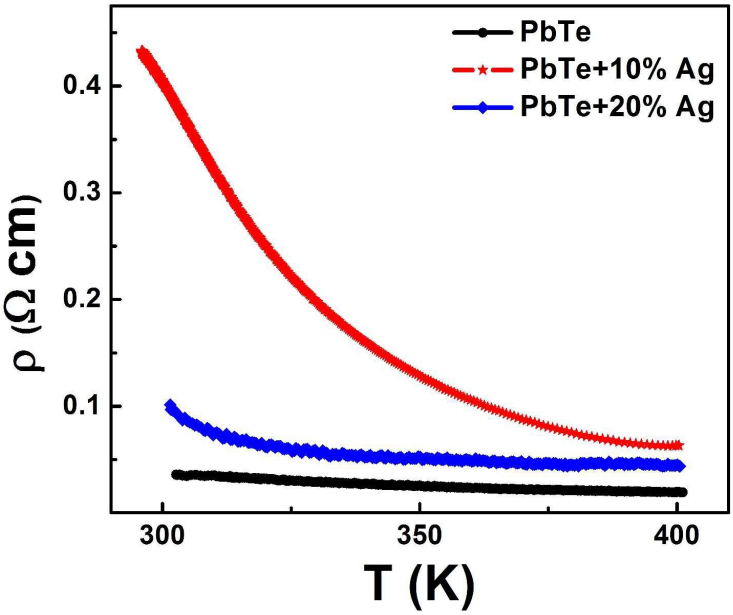

(b)

Figure 9. (a) Thermoelectric power and (b) Electrical resistivity of PbTe, PbTe:10Ag and PbTe:20Ag thin films

The temperature dependence of the electrical resistivity (ρ) in the temperature range of 300 K to 400 K for PbTe, PbTe:10Ag and PbTe:20Ag films are shown in Figure 9(b). For all the samples, electrical resistivity decreases with increasing temperature showing the behavior of a semiconductor. Furthermore, the resistivity of Ag added PbTe is found to be greater than the

PbTe. The Power factors ($F = S^2/\rho$) for PbTe, PbTe:10Ag and PbTe:20Ag films in the temperature of 300 K to 400 K are shown in Figure 10(a). Although the thermoelectric power of the Ag added thin films is higher than the PbTe, the power factor of Ag added thin films is lower than that of the PbTe thin film due to its high electrical resistivity in the same temperature range. Carrier concentration and hall mobility of the films measured at room temperature for all three thin films are shown in Figure 10(b).

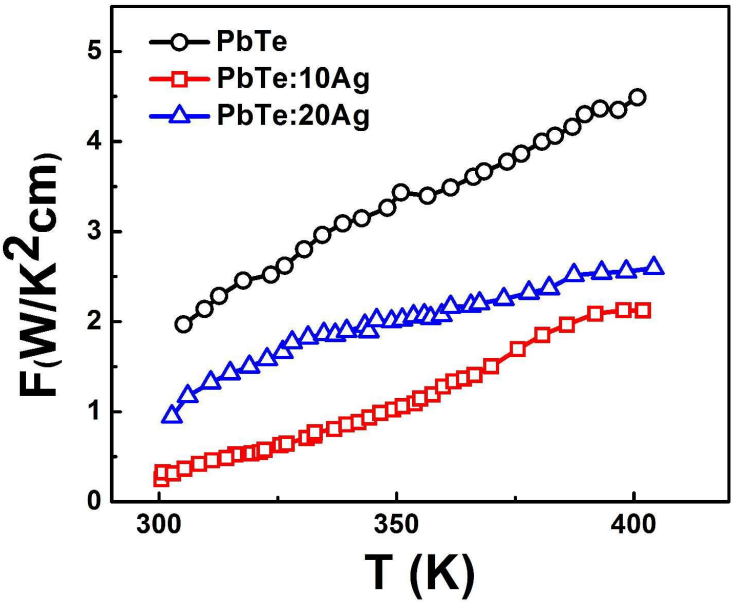

(a)

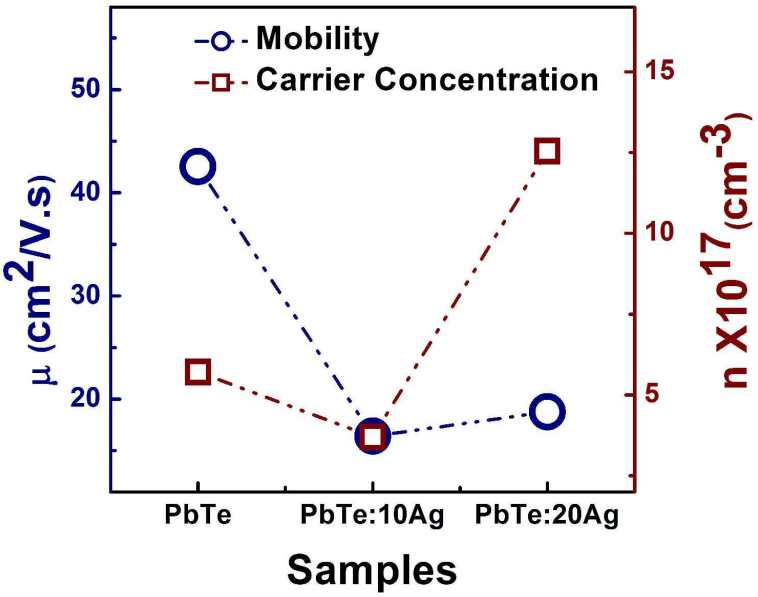

(b)

Figure 10. (a) Power Factor, (b) Carrier mobility and concentration of PbTe, PbTe:10Ag and PbTe:20Ag thin films

In case of PbTe:10Ag thin film, both carrier concentration and mobility decrease and leading to increase in the resistivity ($\rho=1/ne\mu$). But in PbTe:20Ag, an increase in carrier concentration as well as mobility have cooperatively decreased the electrical resistivity in comparison to PbTe:10Ag thin film. thin films. The random distribution of nanostructures formed at the surface for Ag added PbTe thin films is likely to cause the reduction in carrier mobility as compared to PbTe. The high electrical resistivity can be reduced by several approaches. One such approach is tuning the size of the nanostructures in PbTe:Ag thin films by thermal annealing in vacuum. This may increase the size of nanostructures and as result of it, the scattering of charge carriers from the boundary of nanostructures decreases, leading to the decrease in electrical resistivity. Similar mechanism may result with ion beam irradiation but it may also generate defects which can be annealed out during thermal annealing. Since electrical resistivity of PbTe films increase up to 2-3 order of magnitude after exposing in air[23], capping the surface may also ensure reduction in absorption of O and thus reduction in resistivity. Apart from these approaches, depositing thick films of PbTe:Ag can lead to reduction in electrical resistivity. Patil et al[24] showed that resistivity decreases sharply with film thickness from 50 nm up to 150 nm and then it saturates for higher thickness. This is because, with the increase in film thickness grain size increases which results in increase in carrier mobility and decrease in electrical resistivity.

The physical mechanism responsible for thermoelectric power enhancement is proposed to be due to grain-boundary potential barrier scattering. Figure 11 schematically represents the mechanism of energy filtering of charge carriers by the potential barrier formed at the interfaces of nanostructures where W is the width of the potential barrier, which is equal to the size of the nanocomposite [15]. This energy barrier formed at the interfaces of nanostructures (E_b) obstruct the low energy charge carriers to take part in the transport process and act as additional scattering centers, resulting in the high electrical resistivity for PbTe:10Ag thin film. The charge carriers having energy lower than E_b (red circle in Figure 11) get trapped along the grain interfaces, whereas, the charge carriers with higher energy than E_b (green circle in Figure 11) move freely. With the increases in temperature (from 300 K to 400 K), more charge carriers gain energy to overcome the energy barrier resulting in a decrease in electrical resistivity. Energy filtering of charge carriers increases the average energy of the carriers taking part in the transport process.

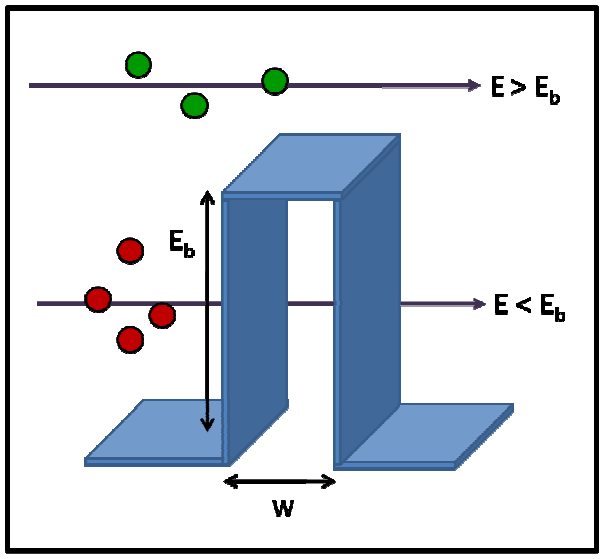

Figure 11. Schematic representation for the mechanism of charge transport across the nanocomposite interfaces of the sample. Red and green circles represent the low and high energy charge carriers at the grain boundaries.

The value of thermoelectric power depends upon the average energy of charge carriers and is inversely related to the carrier concentration, therefore the phenomenon of energy filtering of charge carrier leads to the enhancement in thermoelectric power of PbTe:10Ag thin film by 30% in comparison to the PbTe thin films. The above observation is in good agreement with the results obtained for Ag-incorporated PbTe bulk synthesized via hot-press method [15]. The formation of $Ag_{2-x}Te$ structures in Ag added samples are also responsible for the enhancement in thermoelectric power, as Ag_2Te is reported to be a better thermoelectric material [25]. The thermoelectric power and electrical resistivity of PbTe:20Ag films are lower than PbTe:10Ag thin film. Since, the nanostructures formed on the surface of PbTe:20Ag are smaller in size than PbTe:10Ag thin, therefore the width of the potential barrier is smaller. These nanostructures are connected to each other which results in a small increase in mobility. Besides this, the carrier concentration in PbTe:20Ag film is also increased, therefore as a result of combined effect of increase in carrier concentration and carrier energy filtering by potential barrier, electrical thermoelectric power and resistivity reduces in comparison to PbTe:10Ag thin films.

4. CONCLUSION

The PbTe, PbTe:10Ag and PbTe:20Ag nanocomposites in the form of thin films were synthesized by thermal evaporation method. AFM and SEM images showed a major change in surface morphology for Ag added PbTe thin films. Island like nanostructures are formed on the surface due to the presence Pb inclusions, which precipitated out due to the formation of Ag-Te Alloy. The XRD results show increase in crystallinity in Ag added samples and also indicate the presence of $Ag_{2-x}Te$ alloy which was further confirmed by XPS. Thermoelectric power of PbTe:10Ag and PbTe:20Ag were found to be ~30 % and 10 % higher than PbTe thin film respectively. Power factor is decreased in Ag added PbTe thin film due to increase in electrical resistivity. The increase in thermoelectric power is attributed to increase in scattering centers which obstruct the low energy charge carriers to take part in the transport process. The phenomenon of carrier energy filtering leads to the enhancement of thermoelectric power in this system.

ACKNOWLEDGEMENT

One of the authors (Manju Bala) is grateful to the Council for Scientific and Industrial Research (CSIR) for providing financial support in the form of fellowship. The authors are grateful to the Department of Science and Technology (New Delhi) for providing the SEM under the Nano Mission Project and XRD system at IUAC under the IRHPA project to boost the research activities. The authors would like to thank Mrs. Indra Sulania, Dr. Saif A Khan, Mr.Sunil Ojha, and Dr. Pawan K. Kulriya for their help in various analysis and discussion. The authors thank Mr. Santosh Choudhury, IOP Bhubaneswar for XPS measurements.

AUTHORS INFORMATION

Corresponding authors

Manju Bala and K. Asokan

*E-mail: manjubala474@gmail.com, asokaniuac@gmail.com,

Inter-University Accelerator Centre, Vasant Kunj, New Delhi, 110067, INDIA

Phone no. +918745037342

Authors Contribution

This manuscript was written based on contributions from all authors. All authors have given approval to the final version of the manuscript.

REFERENCES

1. Rowe, D. M., *CRC handbook of thermoelectrics*. CRC press: **1995**.
2. Bode, D. E.; Levinstein, H., Effect of oxygen on the electrical properties of lead telluride films. *Physical Review* **1954,** *96* (2), 259.
3. Snyder, G. J.; Toberer, E. S., Complex thermoelectric materials. *Nature materials* **2008,** *7* (2), 105-114.
4. Tritt, T. M.; Subramanian, M., Thermoelectric materials, phenomena, and applications: a bird's eye view. *MRS bulletin* **2006,** *31* (03), 188-198.
5. Martin, J.; Wang, L.; Chen, L.; Nolas, G., Enhanced Seebeck coefficient through energy-barrier scattering in PbTe nanocomposites. *Physical Review B* **2009,** *79* (11), 115311.
6. Faleev, S. V.; Léonard, F., Theory of enhancement of thermoelectric properties of materials with nanoinclusions. *Physical Review B* **2008,** *77* (21), 214304.
7. LaLonde, A. D.; Pei, Y.; Snyder, G. J., Reevaluation of PbTe1− xIx as high performance n-type thermoelectric material. *Energy & Environmental Science* **2011,** *4* (6), 2090-2096.
8. Heremans, J. P.; Jovovic, V.; Toberer, E. S.; Saramat, A.; Kurosaki, K.; Charoenphakdee, A.; Yamanaka, S.; Snyder, G. J., Enhancement of thermoelectric efficiency in PbTe by distortion of the electronic density of states. *Science* **2008,** *321* (5888), 554-557.
9. JeffreyáSnyder, G., High thermoelectric figure of merit in heavy hole dominated PbTe. *Energy & Environmental Science* **2011,** *4* (6), 2085-2089.
10. Pei, Y.; Shi, X.; LaLonde, A.; Wang, H.; Chen, L.; Snyder, G. J., Convergence of electronic bands for high performance bulk thermoelectrics. *Nature* **2011,** *473* (7345), 66-69.
11. Tavrina, T.; Rogacheva, E.; Pinegin, V., Structural, thermoelectric and galvanomagnetic properties of PbTe-BiTe semiconductor solid solutions. *Mold. J. Phys. Sci* **2005,** *4* (4), 430-434.
12. Heremans, J. P.; Thrush, C. M.; Morelli, D. T., Thermopower enhancement in PbTe with Pb precipitates. *Journal of Applied Physics* **2005,** *98* (6), 063703.
13. Noda, Y.; Orihashi, M.; Nishida, I. A., Thermoelectric properties of p-type lead telluride doped with silver or potassium. *Materials transactions-JIM* **1998,** *39* (5), 602-605.
14. Dow, H.; Oh, M.; Kim, B.; Park, S.; Min, B.; Lee, H.; Wee, D., Effect of Ag or Sb addition on the thermoelectric properties of PbTe. *Journal of Applied Physics* **2010,** *108* (11), 113709.
15. Hicks, L.; Harman, T.; Sun, X.; Dresselhaus, M., Experimental study of the effect of quantum-well structures on the thermoelectric figure of merit. *Physical Review B* **1996,** *53* (16), R10493.
16. Tripathi, T.; Bala, M.; Asokan, K., An experimental setup for the simultaneous measurement of thermoelectric power of two samples from 77 K to 500 K. *Review of Scientific Instruments* **2014,** *85* (8), 085115.
17. Wang, Z.; Wang, J.; Jeurgens, L.; Mittemeijer, E., Thermodynamics and mechanism of metal-induced crystallization in immiscible alloy systems: Experiments and calculations on Al/a-Ge and Al/a-Si bilayers. *Physical Review B* **2008,** *77* (4), 045424.
18. Yang, Y.; Kung, S.; Taggart, D.; Xiang, C.; Yang, F.; Brown, M.; Kruse, T.; Hemminger, J.; Penner, R., Synthesis of PbTe nanowire arrays using lithographically patterned nanowire electrodeposition. *Nano letters* **2008,** *8* (8), 2447-2451.

19. Wu, H.; Cao, C.; Si, J.; Xu, T.; Zhang, H.; Wu, H.; Chen, J.; Shen, W.; Dai, N., Observation of phonon modes in epitaxial PbTe films grown by molecular beam epitaxy. *Journal of Applied Physics* **2007,** *101* (10), 103505-103505-5.
20. Samal, A.; Pradeep, T., Room-temperature chemical synthesis of silver telluride nanowires. *The Journal of Physical Chemistry C* **2009,** *113* (31), 13539-13544.
21. Heremans, J., Low-dimensional thermoelectricity. *ACTA PHYSICA POLONICA SERIES A* **2005,** *108* (4), 609.
22. Ito, M.; Seo, W.-S.; Koumoto, K., Thermoelectric properties of PbTe thin films prepared by gas evaporation method. *Journal of materials research* **1999,** *14* (01), 209-212.
23. Das, V. D.; Bhat, K. S., Electrical conductivity of air-exposed and unexposed lead telluride thin films-temperature and size effects. *Journal of Physics D: Applied Physics* **1989,** *22* (1), 162.
24. Patil, S.; Pawar, P., STRUCTURAL AND THERMOELECTRIC PROPERTIES OF THERMALLY EVAPORATED PbTe THIN FILMS. *Chalcogenide letters* **2012,** *9* (4), 133-143.
25. Taylor, P.; Wood, C., Thermoelectric properties of Ag2Te. *Journal of Applied Physics* **1961,** *32* (1), 1-3.

Colour Graphic:

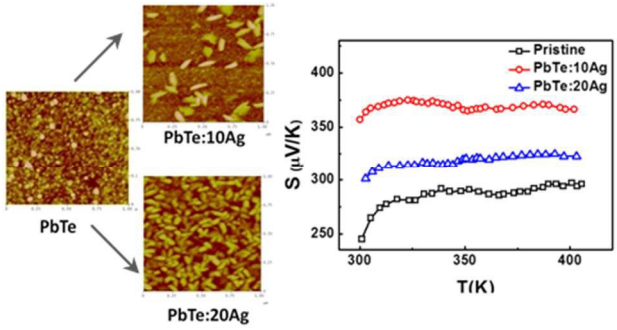

Novelty of the work:

Formation of nanostructures results in the enhancement in thermoelectric power of PbTe:Ag thin films